World Journal of Gastroenterology

Submit a Manuscript: https://www.f6publishing.com

World J Gastroenterol 2023 March 14; 29(10): 1602-1613

DOI: 10.3748/wjg.v29.i10.1602

ISSN 1007-9327 (print) ISSN 2219-2840 (online)

ORIGINAL ARTICLE

Retrospective Study

Quantitative parameters in novel spectral computed tomography: Assessment of Ki-67 expression in patients with gastric adenocarcinoma

Li-Ting Mao, Wei-Cui Chen, Jian-Ye Lu, Han-Liang Zhang, Yong-Song Ye, Yu Zhang, Bo Liu, Wei-Wei Deng, Xian Liu

Specialty type: Gastroenterology and hepatology

Provenance and peer review: Unsolicited article; Externally peer reviewed.

Peer-review model: Single blind

Peer-review report's scientific quality classification

Grade A (Excellent): 0
Grade B (Very good): B, B
Grade C (Good): 0
Grade D (Fair): 0
Grade E (Poor): 0

P-Reviewer: Shariati MBH, Iran; Vorobjova T, Estonia

Received: August 29, 2022
Peer-review started: August 29, 2022
First decision: December 12, 2022
Revised: December 23, 2022
Accepted: January 16, 2023
Article in press: January 16, 2023
Published online: March 14, 2023

Li-Ting Mao, Wei-Cui Chen, Jian-Ye Lu, Han-Liang Zhang, Yong-Song Ye, Bo Liu, Xian Liu, Department of Radiology, The Second Affiliated Hospital of Guangzhou University of Chinese Medicine, Guangzhou 510120, Guangdong Province, China

Yu Zhang, Department of Pathology, The Second Affiliated Hospital of Guangzhou University of Chinese Medicine, Guangzhou 510120, Guangdong Province, China

Wei-Wei Deng, Department of Scientific Research, Clinical & Technical Support, Philips Healthcare China, Shanghai 200040, China

Corresponding author: Xian Liu, PhD, Professor, Department of Radiology, The Second Affiliated Hospital of Guangzhou University of Chinese Medicine, No. 111 Dade Road, Yuexiu District, Guangzhou 510120, Guangdong Province, China. liuxian74@hotmail.com

Abstract

BACKGROUND

The level of Ki-67 expression has served as a prognostic factor in gastric cancer. The quantitative parameters based on the novel dual-layer spectral detector computed tomography (DLSDCT) in discriminating the Ki-67 expression status are unclear.

AIM

To investigate the diagnostic ability of DLSDCT-derived parameters for Ki-67 expression status in gastric carcinoma (GC).

METHODS

Dual-phase enhanced abdominal DLSDCT was performed preoperatively in 108 patients with gastric adenocarcinoma. Primary tumor monoenergetic CT attenuation value at 40-100 kilo electron volt (kev), the slope of the spectral curve (λ_{HU}), iodine concentration (IC), normalized IC (nIC), effective atomic number (Z^{eff}) and normalized Z^{eff} (nZ^{eff}) in the arterial phase (AP) and venous phase (VP) were retrospectively compared between patients with low and high Ki-67 expression in gastric adenocarcinoma. Spearman's correlation coefficient was used to analyze the association between the above parameters and Ki-67 expression status. Receiver operating characteristic (ROC) curve analysis was performed to compare

the diagnostic efficacy of the statistically significant parameters between two groups.

RESULTS

Thirty-seven and 71 patients were classified as having low and high Ki-67 expression, respectively. $CT_{40\ kev\text{-}VP}$, $CT_{70\ kev\text{-}VP}$, $CT_{100\ kev\text{-}VP}$, and Z^{eff}-related parameters were significantly higher, but IC-related parameters were lower in the group with low Ki-67 expression status than the group with high Ki-67 expression status, and other analyzed parameters showed no statistical difference between the two groups. Spearman's correlation analysis showed that $CT_{40\ kev\text{-}VP}$, $CT_{70\ kev\text{-}VP}$, $CT_{100\ kev\text{-}VP}$, Z^{eff}, and n Z^{eff} exhibited a negative correlation with Ki-67 status, whereas IC and nIC had positive correlation with Ki-67 status. The ROC analysis demonstrated that the multi-variable model of spectral parameters performed well in identifying the Ki-67 status [area under the curve (AUC) = 0.967; sensitivity 95.77%; specificity 91.89%)]. Nevertheless, the differentiating capabilities of single-variable model were moderate (AUC value 0.630 - 0.835). In addition, the nZ^{eff}_{VP} and nIC_{VP} (AUC 0.835 and 0.805) showed better performance than $CT_{40\ kev\text{-}VP}$, $CT_{70\ kev\text{-}VP}$ and $CT_{100\ kev\text{-}VP}$ (AUC 0.630, 0.631 and 0.662) in discriminating the Ki-67 status.

CONCLUSION

Quantitative spectral parameters are feasible to distinguish low and high Ki-67 expression in gastric adenocarcinoma. Z^{eff} and IC may be useful parameters for evaluating the Ki-67 expression.

Key Words: Spectral computer tomography; Quantitative parameters; Gastric carcinoma; Iodine concentration; Effective atomic number; Ki-67 expression

Core Tip: This is a retrospective study to preoperatively distinguish the expression of Ki-67 index based on the parameters of spectral computer tomography (CT) in patients with gastric adenocarcinoma. The CT attenuation of virtual monoenergetic images in venous phase and effective atomic number were negatively related to the expression of Ki-67, while iodine concentration exhibited positive associations with it. Multi-variable model of spectral parameters exhibited a better diagnostic efficiency than other single-variable model of spectral parameter in discriminating low and high Ki-67 expression in gastric adenocarcinoma.

Citation: Mao LT, Chen WC, Lu JY, Zhang HL, Ye YS, Zhang Y, Liu B, Deng WW, Liu X. Quantitative parameters in novel spectral computed tomography: Assessment of Ki-67 expression in patients with gastric adenocarcinoma. *World J Gastroenterol* 2023; 29(10): 1602-1613
URL: https://www.wjgnet.com/1007-9327/full/v29/i10/1602.htm
DOI: https://dx.doi.org/10.3748/wjg.v29.i10.1602

INTRODUCTION

Gastric carcinoma (GC) is the fifth commonest malignancy and the fourth most predominant cause of cancer-related mortality worldwide according to the Global Cancer Statistics 2020[1]. Although the global age-standardized rates of incidence and mortality presented a slight decrease from 1990 to 2019, China had a high incidence-mortality ratio (0.845) and five-year prevalence (27.6/100 000)[2]. A large number of GC cases are found at the advanced stage and have a relatively poor prognosis, with an overall survival rate of 25% worldwide[3]. The high proportion of tumor metastasis, intratumor heterogeneity and chemotherapeutic resistance leads to unfavorable survival outcomes in patients with GC. Conventionally, the tumor-node-metastasis (TNM) stage, histologic classification and differentiation are the major prognostic indicators for GC[4]. In addition, some oncogenic protein markers, such as antigen Ki-67, have been associated with the prognosis of GC patients[5].

Cell proliferation is a distinguishing feature of cancer. The Ki-67 protein, a nucleus-associated antigen, which is a convenient and reproducible biomarker in this process, is expressed during the cell proliferation cycle including G1, S, G2, and mitosis phases[6]. Some studies have demonstrated that Ki-67 proliferation index could be a potential indicator to predict the prognosis and identify high-risk GC cases, and was relevant to TNM stage, tumor differentiation grade, invasion depth and distant metastasis[5,7,8]. Additionally, Ki-67 index was associated with chemotherapy efficacy in the advanced GC, because cytotoxic chemotherapeutic drugs are effective against tumor cells that have entered the cell division cycle. Thus, identifying the Ki-67 status noninvasively would be beneficial for predicting

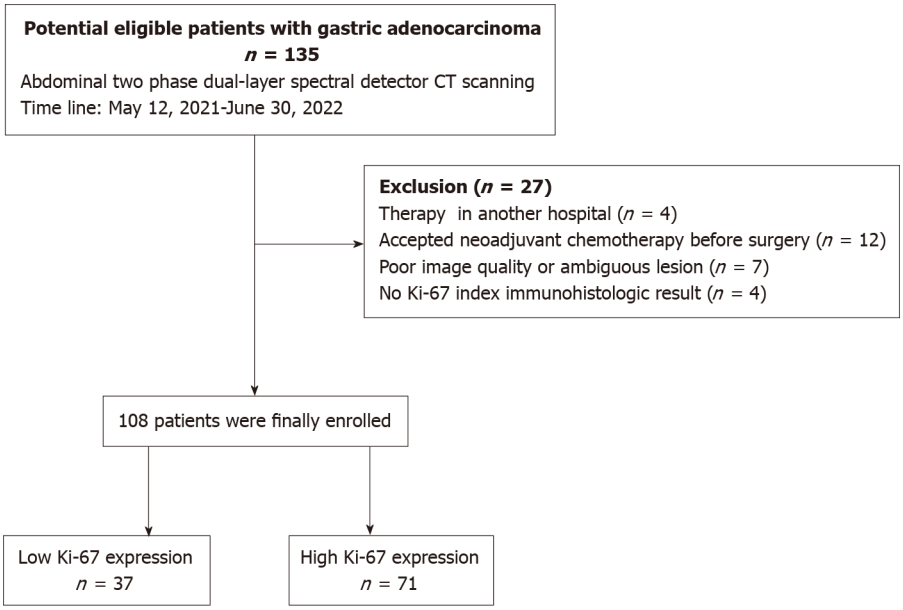

DOI: 10.3748/wjg.v29.i10.1602

Figure 1 The flow chart of the process of patient selection. CT: Computed tomography.

the prognosis and chemotherapeutic response in the patients with GC.

Recently, a novel dual-layer spectral detector CT (DLSDCT), which utilizes a detector-based dual-energy separation technology to acquire low- and high-energy data synchronously with two layers of detectors, makes for beam-hardening rectification, material decomposition, and image de-noising[9,10]. This system applies projection-space decomposition and generates various spectral basis images (SBIs) except for the conventional polyenergetic images, including material-specific images [iodine concentration (IC) images, virtual non-contrast images, effective atomic number (Z^{eff}) images] and energy-specific images [virtual monoenergetic images (VMIs)]. These spectral images are widely used for enhancing image contrast, improving lesion detection, characterizing materials, reducing artifact, and lowering radiation dosage[9-12]. Some studies have investigated the gastric lesions based on the IC derived from dual-energy spectral CT, such as distinguishing between malignant and benign gastric mucosal lesions[13], diagnosing GC and its histological type[14], and detecting serosal invasion of GC [15]. The latest study demonstrated that virtual monochromatic CT values were related to proliferative activity of tumor cells[16]. The Z^{eff} was correlated with Ki-67 expression in laryngeal squamous cell carcinoma[17], and could predict the vascular density of affected lesions[18]. However, only a few studies have applied the quantitative parameters [IC and normalized IC (nIC)] from spectral CT to evaluate the Ki-67 expression status in patients with gastric adenocarcinoma, but not including the CT attenuation value and Z^{eff} derived from the novel DLSDCT. Thus, the aim of this study is to explore the clinical usefulness of the quantitative parameters of novel DLSDCT in assessing the Ki-67 expression status in patients with gastric adenocarcinoma.

MATERIALS AND METHODS

Patients

This retrospective study was approved by Institutional Review Board of our hospital, with a waiver for written informed consent. From May 2021 to June 2022, 135 patients diagnosed with gastric adenocarcinoma through endoscopic biopsy underwent non-contrast and contrast-enhanced CT scans on a DLSDCT scanner (IQon Spectral CT, Philips Healthcare, Best, The Netherlands). Twenty-eight cases were excluded for the following factors: (1) Transferred to another hospital for further treatment (n = 4); (2) Accepted or required neo-adjuvant chemotherapy prior to surgery (n = 12); (3) Poor image quality or the lesion is ambiguous on the image (n = 7); or (4) Lack of the Ki-67 index immunohistologic result (n = 4). Finally, 108 patients were analyzed in this study. The detailed procedure of patient selection is shown in Figure 1.

Spectral CT imaging protocol

The interval between the DLSDCT examination and surgery was less than one week. Before CT examination, patients were required to be fast for 6-8 h and drank 800-1000 mL of water. The scan ranged from the diaphragm to the symphysis pubis in a supine position and cranio-caudal direction.

Nonionic contrast agent (Ultravist, Byer HealthCare) (370 mg/mL, 80 mL) was injected intravenously at a flow rate of 2.5 mL/s, with an automated injector (Stellant, Medrad, Byer HealthCare), following 30 mL of normal saline flushing at the same flow rate. Using bolus-tracking technique, the arterial phase (AP) scan was triggered at a threshold of 200 hounsfield unit (HU) and an additional delay of 6 s. The venous phase (VP) images were respectively collected at 35 s after injecting the contrast agent.

CT scan parameters were as follows: Tube voltage 120 kVp, automatic tube current 37-84 mAs, detector collimation 64 mm × 0.625 mm, reconstruction matrix 512 × 512. Conventional and SBI were reconstructed using the iDose 4 algorithm (Philips Healthcare). All CT images were reconstructed with a slice thickness of 1 mm and an increment of 1 mm, using a standard kernel. All image data were transferred to a workstation (IntelliSpace Portal, version 10.1, Philips Healthcare) for post-processing and analysis.

Image analysis

The image analysis was conducted by two gastrointestinal radiologists (reader 1 and reader 2, with 10 and 26 years of experience, respectively), who were blind to pathological results. The two-dimensional region-of-interest (ROI) was drawn on lesion manually, according to the following principles: (1) Polygon ROIs covered the enhanced areas of the lesions as much as possible; (2) Be careful to avoid the areas of necrosis, calcification, and vessels; (3) All lesions were measured on three consecutive axial layers by the same evaluator, and average values were calculated; and (4) The size, form, and position of the ROIs were maintained consistent between two phases images, by applying the copy-and-paste function of the workstation. A circular ROI was placed in the abdominal aorta parallel with lesion. The intraclass correlation coefficient (ICC) between the two radiologists was calculated. The final results of all ROIs were measured by the radiologist with 10 years' experience.

The following quantitative spectral parameters were automatically calculated using the post-processing software: The CT attenuation values of monochromatic images [40 kilo electron volt (kev), 70 kev and 100 kev], IC, and the Z^{eff}. Additionally, three related parameters were measured: (1) The nIC was computed as Nic = IC_{lesion}/IC_{aorta}, where IC_{lesion} and IC_{aorta} are the ICs of the lesions and abdominal aorta, which help to minimize individual variation; (2) The normalized Z^{eff} (nZ^{eff}) was counted similarly to nIC, $nZ^{eff} = Z^{eff}_{lesion}/Z^{eff}_{aorta}$; and (3) The slope of the spectral curve (λ_{HU}) was calculated as the CT attenuation values, $\lambda_{HU} = (CT_{40\,kev} - CT_{70\,kev})/30$, where $CT_{40\,kev}$ and $CT_{70\,kev}$ are the attenuation of the tumors at 40 kev and 70 kev monochromatic images, respectively[19]. Two phases (AP and VP) of CT attenuation value, IC, nIC, Z^{eff}, nZ^{eff}, and λ_{HU} were measured.

Histopathology evaluation

A pathologist with 22 years of experience (Yu Zhang) conducted the pathologic analysis. The TNM staging was determined on the basis of the American Joint Committee on Cancer (AJCC) 8th manual of gastric cancer[20]. The Ki-67 proliferation index was evaluated according to the normal immunohistochemistry process and evaluated by the pathologist blindly. The Ki-67 polyclonal antibody used (Roche #) was produced by Shanghai Rebiosci Biotech Co., Ltd. The specimens were analyzed in a high power field (× 400). The pathologist selected five fields of view randomly and each region was observed. Then 100 cells were selected in each field and the number and intensity of positively stained cells were counted. Finally, an average number of five fields were recorded. The Ki-67 indexes were categorized as low expression (< 50% positive cells) or high expression (≥ 50% positive cells), according to relevant reports[7,21].

Statistical analysis

Statistical analysis was performed using MedCalc Statistical Software version 19.4.1 (MedCalc Software, Ostend, Belgium; https://www.medcalc.org; 2020). Continuous variables were presented as the mean ± SD, and categorical variables as proportions. ICC analyses were performed with the data of 20 patients to evaluate the reliability of spectral parameters measurement. An ICC > 0.75 was considered good.

The Shapiro-Wilk test was used to test the normality of data distributions. The Student's *t*-test was employed to analyze the differences in clinical demographics and imaging parameters between low and high Ki-67 expressing status. Spearman's correlation coefficient was used to assess the correlation between the quantitative imaging parameters and the Ki-67 expression status.

Receiver operating characteristic (ROC) analysis was performed to evaluate the diagnostic efficacy in classifying Ki-67 statuses. Area under the curve (AUC) and their 95% confidence intervals (CIs) were determined using unstratified bootstrap replicates 10 000 times. The optimal cutoff value was determined according to the Youden index. The difference between ROC curves were evaluated by pairwise comparison test. A two-sided *P* value of less than 0.05 was regarded statistically significant.

Table 1 Inter-reader agreement of spectral parameters measurement

Parameters	ICC (95%CI)	
	AP	VP
Z^{eff}_{lesion}	0.88 (0.71, 0.95)	0.86 (0.69, 0.94)
Z^{eff}_{aorta}	0.94 (0.85, 0.97)	0.95 (0.88, 0.98)
IC_{lesion} (mg/mL)	0.86 (0.56, 0.95)	0.87 (0.73, 0.95)
IC_{aorta} (mg/mL)	0.98 (0.94, 0.99)	0.95 (0.86, 0.98)
$CT_{40\ kev}$ (HU)	0.95 (0.88, 0.98)	0.96 (0.79, 0.99)
$CT_{70\ kev}$ (HU)	0.92 (0.78, 0.97)	0.91 (0.50, 0.98)
$CT_{100\ kev}$ (HU)	0.86 (0.69, 0.94)	0.89 (0.70, 0.96)

ICC: Intraclass correlation coefficient; Z^{eff}_{lesion} and Z^{eff}_{aorta}: The effective atomic number of lesion and aorta; $CT_{40\ kev}$, $CT_{70\ kev}$ and $CT_{100\ kev}$: The computed tomography attenuation value of 40 kilo electron volt (kev), 70 kev and 100 kev monochromatic images; IC_{lesion} and IC_{aorta}: The iodine concentration of lesion and aorta; HU: Hounsfield unit; AP: Arterial phase; VP: Venous phase; 95%CI: 95% confidence interval.

RESULTS

Patient demographics and histopathological findings

A total of 108 patients (mean age 61.9 years, range 34-85 years) were analyzed, consisting of 46 females and 62 males. The gastric tumors were located in the antrum in 48 cases (44.4%), in the corpus in 24 cases (22.2%), in the fundus in 11 cases (10.1%), in the antrum and corpus in 9 cases (8.3%), in the gastric angle in 9 cases (8.3%), and in the cardia in 7 case (6.4%).

Referring to the pathologic TNM staging of GC (AJCC 8th edition), 27 patients had gastric cancer of less than stage pT2, 32 patients had stage pT3 gastric cancer, and 49 patients had stage T4 gastric cancer. Twenty-six patients had no regional lymph node metastasis, whereas 24 patients had less than three lymph nodes invaded (pN1), 30 patients had 3-6 regional lymph nodes invaded (pN2), and 28 patients had seven or more regional lymph nodes invaded (pN3). The immunohistochemical staining results revealed that 37 cases were categorized as having low expression of the Ki-67, while 71 cases were categorized as having high expression. According to the World Health Organization grading criteria, 29 (26.8%) and 79 (73.1%) tumors were respectively classified as moderately and poorly differentiated adenocarcinoma.

Reliability of measurements

The ICC values for Z^{eff}_{lesion}, Z^{eff}_{aorta}, IC_{lesion}, IC_{aorta}, $CT_{40\ kev}$, $CT_{70\ kev}$, $CT_{100\ kev}$ in AP and VP were all more than 0.85, and the specific values are shown in Table 1.

Correlation between spectral parameters and Ki-67 status

Z^{eff} and nZ^{eff} in AP and VP presented a moderate negative correlation with Ki-67 status ($P < 0.001$), whereas the IC and nIC in AP and VP were moderately positive-correlated with Ki-67 status ($P < 0.001$). The $CT_{40\ kev\text{-}VP}$, $CT_{70\ kev\text{-}VP}$ and $CT_{100\ kev\text{-}VP}$ were weakly negative-correlated with Ki-67 status (all $P < 0.05$). However, the $CT_{40\ kev\text{-}AP}$, $CT_{70\ kev\text{-}AP}$, $CT_{100\ kev\text{-}AP}$ and $\lambda_{HU\text{-}AP}$ and $\lambda_{HU\text{-}VP}$ were not correlated with Ki-67 expression (all $P > 0.05$). The correlation coefficients and 95%CIs are shown in Table 2.

Comparison of spectral parameters between different Ki-67 status

Table 3 and Figure 2 show the results of quantitative analysis. Compared with high Ki-67 status, the low Ki-67 status had higher Z^{eff}_{AP}, Z^{eff}_{VP}, nZ^{eff}_{AP}, nZ^{eff}_{VP}, $CT_{40\ kev\text{-}VP}$, $CT_{70\ kev\text{-}VP}$ and $CT_{100\ kev\text{-}VP}$, and had lower IC_{AP}, IC_{VP}, nIC_{AP} and nIC_{VP}. Although the $CT_{40\ kev\text{-}AP}$, $CT_{70\ kev\text{-}AP}$ and $CT_{100\ kev\text{-}AP}$ of low Ki-67 status were slightly higher than that of high Ki-67 status, it was not statistically significant. Similarly, no significant differences were found in the λ_{HU} of AP and VP between the two groups. Figures 3 and 4 show the spectral parameter images of two cases with high and low Ki-67 expression, respectively.

Diagnostic performance

Table 4 summarizes the results of ROC analysis for evaluating the diagnostic performance of 12 significant spectral parameters in discriminating the Ki-67 status. For diagnosing the high Ki-67 labeling index, the Z^{eff}, nZ^{eff}, IC and nIC in AP and VP performed moderate efficiency (AUC value, ranged from 0.747 to 0.835), and there were no significant differences among the AUC values of these parameters. Nevertheless, the $CT_{40\ kev\text{-}VP}$, $CT_{70\ kev\text{-}VP}$, and $CT_{100\ kev\text{-}VP}$ showed general differentiating capabilities (AUC value 0.630, 0.631, 0.662, respectively) in differentiating low from high Ki-67 expression in GC, and the

Table 2 Correlation between spectral parameters and Ki-67 status

Parameters		Ki-67 status	
		r (95%CI)	*P* value
AP	$CT_{40\ kev}$	-0.162 (-0.362, 0.043)	0.093
	$CT_{70\ kev}$	-0.097 (-0.290, 0.102)	0.316
	$CT_{100\ kev}$	-0.074 (-0.277, 0.117)	0.449
	λ_{HU}	-0.137 (-0.328, 0.056)	0.156
	Z^{eff}	-0.427 (-0.606, -0.208)	< 0.001
	nZ^{eff}	-0.487 (-0.649, -0.318)	< 0.001
	IC	0.409 (0.228, 0.567)	< 0.001
	nIC	0.449 (0.288, 0.598)	< 0.001
VP	$CT_{40\ kev}$	-0.213 (-0.397, -0.005)	0.027
	$CT_{70\ kev}$	-0.216 (-0.407, -0.004)	0.025
	$CT_{100\ kev}$	-0.266 (-0.438, -0.096)	0.005
	λ_{HU}	-0.090 (-0.278, 0.093)	0.354
	Z^{eff}	-0.455 (-0.647, -0.215)	< 0.001
	nZ^{eff}	-0.555 (-0.692, -0.403)	< 0.001
	IC	0.405 (0.223, 0.571)	< 0.001
	nIC	0.502 (0.355, 0.651)	< 0.001

Z^{eff}_{AP} and Z^{eff}_{VP}: The effective atomic number in the arterial and venous phase; nZ^{eff}_{AP} and nZ^{eff}_{VP}: The normalized effective atomic number in the arterial and venous phase; IC_{AP} and IC_{VP}: The iodine concentration in the arterial and venous phase; nIC_{AP} and nIC_{AP}: The normalized iodine concentration in the arterial and venous phase; $CT_{40\ kev}$, $CT_{70\ kev}$ and $CT_{100\ kev}$: The computed tomography attenuation value of 40 kilo electron volt (kev), 70 kev and 100 kev monochromatic images; λ_{HU}: The slope of the spectral curve; HU: Hounsfield unit; AP: Arterial phase; VP: Venous phase; 95%CI: 95% confidence interval.

AUC values of these parameters had no statistical differences. Comparing the AUC values of CT attenuation with that of the Z^{eff}- and IC-related parameters, the AUC value of nZ^{eff}_{AP} was higher than $CT_{40\ kev-VP}$ (0.796 *vs* 0.630, $P = 0.047$), and the AUC values of nZ^{eff}_{VP} and nIC_{VP} were higher than $CT_{40\ kev-VP}$, $CT_{70\ kev-VP}$ and $CT_{100\ kev-VP}$ ($P = 0.02$, 0.01, 0.009 and 0.03, 0.01, 0.02, respectively). In addition, the multivariable model ($CT_{70\ kev-VP}$, nZ^{eff}_{AP}, nZ^{eff}_{VP}, nIC_{AP}, nIC_{VP}) was selected for most powerful parameters by multivariate logistic regression, and the model demonstrated excellent efficiency (AUC = 0.967; sensitivity 95.77%; specificity 91.89%) in discriminating high expression of Ki-67 in GC.

DISCUSSION

The recently developed DLSDCT could quantitatively map the IC and Z^{eff} of the tissue in enhanced images, and offer CT attenuation values on a wide range of VMIs. In this study, we explored the association between quantitative parameters derived from DLSDCT and the Ki-67 labeling index of gastric adenocarcinoma. Our results revealed that the $CT_{40\ kev-VP}$, $CT_{70\ kev-VP}$, $CT_{100\ kev-VP}$, and Z^{eff}-related parameters were significantly higher, but IC-related parameters were lower in the group with low Ki-67 status. Additionally, the $CT_{40\ kev-VP}$, $CT_{70\ kev-VP}$, $CT_{100\ kev-VP}$, and Z^{eff}-related parameters exhibited negative correlations with Ki-67 status, whereas IC-related parameters positively correlated with it. These results were partially in agreement with previous reports that used different spectral CT systems, which demonstrated that IC and nIC were positively associated with Ki-67 status, and the values of nIC were higher in poorly differentiated gastric adenocarcinomas significantly[22,23].

We found a negative correlation between Z^{eff} and Ki-67 labeling index, which is seemingly at variance with a previous study that Z^{eff} was positively correlated with Ki-67 expression in the laryngeal squamous cell carcinoma[17] and invasive breast cancer[24]. Z^{eff} reflects the total atomic numbers of complex or mixture of materials, and has a close relationship with fundamental properties of the elements[25]. Previous research indicated that the evaluation of Z^{eff} could be able to distinguish the different tissues showing similar attenuative properties at given energy[26]. On account of the concentrations of elements (Cl, K, Ca, Ti, Mn, Fe, Co, Cu, and Zn) are lower in the stomach cancerous tissue than normal tissue[25], gastric cancer tissue exhibits a lower Z^{eff} than its healthy counterpart[27]. It is

Table 3 Comparison of dual-layer spectral detector computed tomography-derived parameters between low and high Ki-67 expression status

	Parameters	Low Ki-67 status	High Ki-67 status	*t* value	*P* value
AP	$CT_{40\ kev}$	177.3 ± 43.9	162.3 ± 37.8	1.85	0.068
	$CT_{70\ kev}$	90.9 ± 20.1	85.5 ± 16.6	1.48	0.141
	$CT_{100\ kev}$	63.8 ± 12.7	61.7 ± 12.6	0.81	0.422
	λ_{HU}	2.88 ± 1.04	2.56 ± 0.98	1.58	0.118
	Z^{eff}	8.30 ± 0.19	8.21 ± 0.10	2.87	0.006
	nZ^{eff}	0.78 ± 0.04	0.74 ± 0.03	5.33	< 0.001
	IC (mg/mL)	1.61 ± 0.15	1.73 ± 0.19	-3.53	0.001
	nIC	0.15 ± 0.02	0.19 ± 0.04	-5.88	< 0.001
VP	$CT_{40\ kev}$	265.9 ± 61.4	237.3 ± 45.8	2.50	0.016
	$CT_{70\ kev}$	126.5 ± 33.4	108.0 ± 20.9	3.07	0.003
	$CT_{100\ kev}$	84.3 ± 18.7	73.9 ± 17.2	3.71	0.005
	λ_{HU}	4.65 ± 1.43	4.31 ± 1.15	1.33	0.185
	Z^{eff}	8.75 ± 0.24	8.62 ± 0.15	3.04	0.004
	nZ^{eff}	0.87 ± 0.04	0.83 ± 0.03	6.59	< 0.001
	IC (mg/mL)	2.62 ± 0.17	2.75 ± 0.21	-3.40	0.001
	nIC	0.41 ± 0.04	0.46 ± 0.06	-5.87	< 0.001

$CT_{40\ kev}$, $CT_{70\ kev}$ and $CT_{100\ kev}$: The computed tomography attenuation values of at 40 kilo electron volt (kev), 70 kev and 100 kev respectively; λ_{HU}: The slope of the spectral curve; Z^{eff}: Effective atomic number; nZ^{eff}: The normalized effective atomic number; IC: Iodine concentration; nIC: Normalized iodine concentration; AP: Arterial phase; VP: Venous phase.

known that deficiency or excess of certain essential trace metals is relevant to carcinogenesis of the specific organs[27,28]. The abnormal levels of these elements lead to the discrepancy of toxicity and proliferation activity of cancer cells. We hypothesize that Z^{eff} difference between high and low Ki-67 expression status is more significant due to abnormal metal concentration than tumor heterogeneity and angiogenesis, especially in case of using nZ^{eff}, which eliminate individual differences in hemodynamics.

The blood vessels of tumors are supplied by tumor angiogenesis and invasion of vessels around the tumor. The degree of tumor angiogenesis is strongly linked to tumor growth, progression, and metastasis[29,30]. Wang *et al*[31] found that the degree of CT enhancement is correlated with tumor angiogenesis and the malignancy of the tumor. Compared to CT contrast enhancement, IC can quantitatively indicate the degree of tumor neovascularization and reflect the deposition of iodine in the tissue objectively[32]. In this study, we detected significantly higher IC and nIC values in the AP and VP of the high-expression Ki-67 group, indicating a richer blood supply in these tumors. Compared to IC, the normalized parameter nIC minimized hemodynamic variations between individuals, which could be more comparable among different groups. These findings are consistent with the fact that the high proliferative activity is accompanied by abundant angiogenesis.

In our study, we found no statistical difference in the CT attenuation values at 40-100 kev (at 30 kev interval) in AP between low- and high-expression Ki-67 groups. Likewise, the λ_{HU} of AP and VP between the two groups showed no significant differences, which was different from the result reported by Cheng *et al*[22], who found that the λ_{HU} values were significantly different among the low, medium and high level Ki-67 groups in both VP and delayed phase, and had positive correlation with Ki-67 level. We deemed that the discrepancy might be attributable to the grouping method of Ki-67 index and the constituent ratio of differentiation degree of the analyzed cases was distinct from our study. It is necessary to further explore the usefulness of λ_{HU} values.

When evaluating the diagnostic performance of spectral parameters in discriminating the Ki-67 status, the results from ROC analysis demonstrated that the multi-variable model of spectral parameters performed excellent capacity, with high sensitivity and specificity. In contrast, the single-variable model of Z^{eff}- and IC-related parameters demonstrated moderate efficiency, and 40-100 kev (at 30 kev interval) in VP showed general efficiency. Therefore, the parameters derived from DLSDCT were feasible for the prediction of Ki-67 expression in the gastric adenocarcinoma, which is of great significance in predicting prognosis and guiding treatment for the patients with GC.

Table 4 Receiver operator characteristic analysis of spectral parameters in differentiating Ki-67 low expression status from high expression status

		AUC (95%CI)	TV	YI	Sen (%)	Spe (%)	PPV (%)	NPV (%)	Acc (%)
AP	Z^{eff}	0.759 (0.668, 0.836)	≤ 8.27	0.67	85.92	81.08	92.96	37.84	71.30
	nZ^{eff}	0.796 (0.707, 0.867)	≤ 0.74	0.67	80.28	86.49	85.92	54.05	75.00
	IC	0.752 (0.660, 0.830)	> 1.63	0.60	78.87	81.08	88.73	21.62	65.74
	nIC	0.773 (0.683, 0.848)	> 0.16	0.61	74.65	86.49	81.69	48.65	70.37
VP	$CT_{40\ kev}$	0.630 (0.531, 0.721)	≤ 271.2	0.26	80.28	45.95	95.77	24.32	71.30
	$CT_{70\ kev}$	0.631 (0.533, 0.722)	≤ 138.8	0.31	92.96	37.84	94.37	32.43	73.15
	$CT_{100\ kev}$	0.662 (0.565, 0.750)	≤ 89.3	0.28	81.69	45.95	87.32	32.43	68.52
	Z^{eff}	0.777 (0.687, 0.851)	≤ 8.75	0.73	88.73	83.78	92.96	29.73	74.07
	nZ^{eff}	0.835 (0.751, 0.899)	≤ 0.83	0.68	78.87	89.19	85.92	51.35	74.07
	IC	0.747 (0.654, 0.826)	> 2.65	0.63	84.51	78.38	85.92	27.03	65.74
	nIC	0.805 (0.718, 0.875)	> 0.43	0.71	78.87	91.89	85.92	37.84	69.44
Multi-parameters		0.967 (0.913, 0.992)	-	0.88	95.77	91.89	97.18	86.49	93.52

AUC: Area under the curve; TV: Threshold value; YI: Youden index; Sen: Sensitivity; Spe: Specificity; NPV: Negative predictive value; PPV: Positive predictive value; Acc: Accuracy; Z^{eff}_{AP} and Z^{eff}_{VP}: The effective atomic number in the arterial and venous phase; nZ^{eff}_{AP} and nZ^{eff}_{VP}: The normalized effective atomic number in the arterial and venus phase; IC_{AP} and IC_{VP}: The iodine concentration in the arterial and venous phase; nIC_{AP} and nIC_{AP}: The normalized iodine concentration in the arterial and venous phase; $CT_{40\ kev}$, $CT_{70\ kev}$ and $CT_{100\ kev}$: The computed tomography attenuation values of at 40 kilo electron volt (kev), 70 kev and 100 kev respectively.

There were several limitations in our study. First, this is a retrospective study in which case grouping is not random, hence, an unconscious selection bias may exist. Second, a relatively small number of patients might overstate the consequence of association. Third, the number of cases with different degrees of differentiation was disproportionate, resulting in significance hard to achieve for partially analyzed variables. Fourth, our uniform standard of enhanced scanning protocol with DLSDCT may be different from other centers, thus, the results acquired from other vendors or different scanning parameters may not be directly concluded from our results. It demands further studies to confirm and outspread our preliminary results.

CONCLUSION

Quantitative spectral parameters are feasible to distinguish low and high Ki-67 expression in gastric adenocarcinoma. Multi-variable model of spectral parameters exhibited a better diagnostic efficiency than single-variable model of spectral parameter in discriminating low and high Ki-67 expression in gastric adenocarcinoma. Z^{eff} and IC derived from DLSDCT may be useful parameters for evaluating the Ki-67 proliferation index for gastric adenocarcinoma.

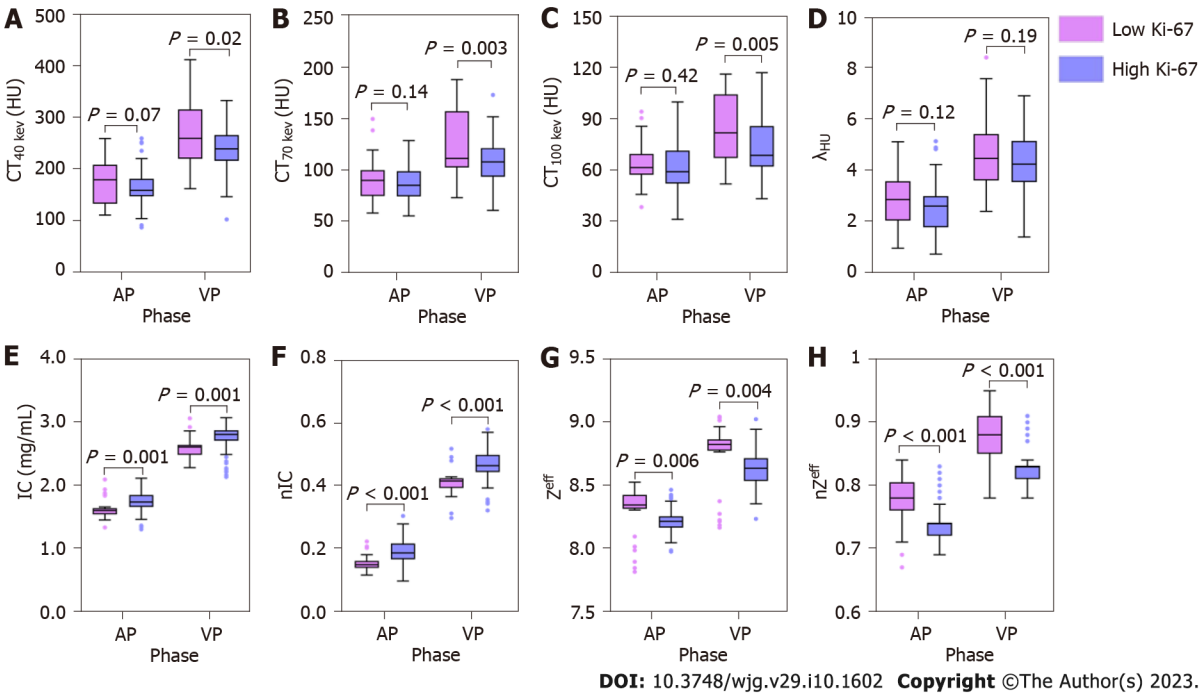

DOI: 10.3748/wjg.v29.i10.1602

Figure 2 Boxplots showing a comparison between low and high Ki-67 expression status demonstrated by computed tomography attenuation value of 40 kilo electron volt, 70 kilo electron volt, 100 kilo electron volt, slope of the spectral curve, iodine concentration, the normalized iodine concentration, effective atomic number, and normalized effective atomic number in both arterial phase and venous phase. A: Computed tomography attenuation value of 40 kev; B: Computed tomography attenuation value of 70; C: Computed tomography attenuation value of 100; D: The slope of the spectral curve; E: Iodine concentration; F: The normalized iodine concentration; G: Effective atomic number; H: Normalized effective atomic number. HU: Hounsfield unit; AP: Arterial phase; VP: Venous phase; IC: Iodine concentration; nIC: The normalized iodine concentration; $CT_{40\ kev}$, $CT_{70\ kev}$ and $CT_{100\ kev}$: The computed tomography attenuation value of 40 kev, 70 kev and 100 kev monochromatic images; Z^{eff}: Effective atomic number; nZ^{eff}: The normalized effective atomic number.

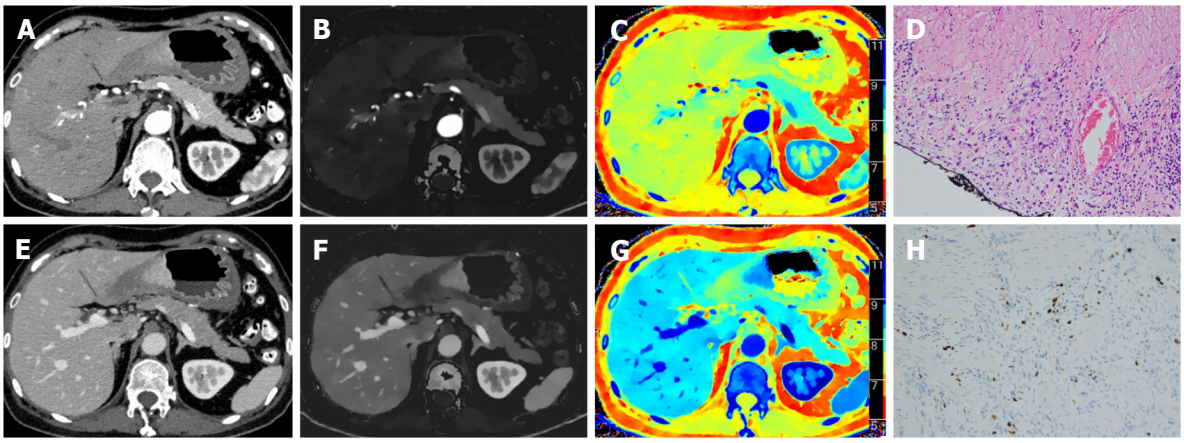

DOI: 10.3748/wjg.v29.i10.1602

Figure 3 A 57-year-old man with gastric adenocarcinoma in the antrum. A: The 70 kilo electron volt (kev) image in arterial phase (AP) show that the computed tomography attenuation value of 70 kev ($CT_{70\ kev}$) value of solid mass is 128.8 HU; B: The iodine map in AP show that the iodine concentration (IC) value of solid mass is 3.44 mg/mL; C: The effective atomic map in AP show that the effective atomic number (Z^{eff}) value of solid mass is 8.25; D: Histologic specimen shows a gastric adenocarcinoma of T4 staging in solid with HE staining (magnification, × 200); E: A 70 kev image in venous phase (VP) show that the CT_{70kev} value of solid mass is 146.9 HU; F: An iodine map in VP show that the IC value of solid mass is 3.32 mg/mL; G: An effective atomic map in VP show that the Z^{eff} value of solid mass is 8.65; H: Ki-67 immunohistochemical staining demonstrated that approximately 80% of cells were positive for nuclear staining (magnification, × 400).

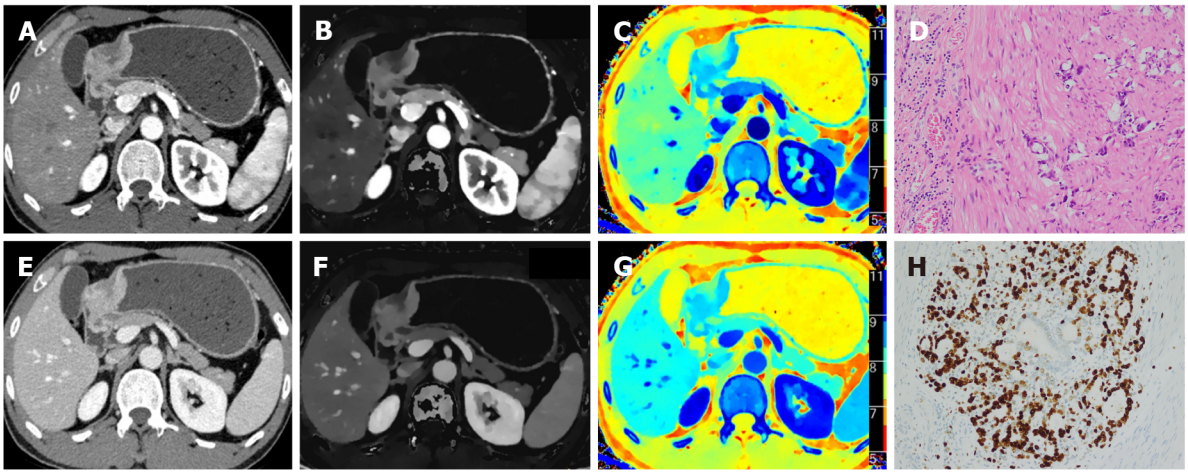

DOI: 10.3748/wjg.v29.i10.1602

Figure 4 A 65-year-old woman with gastric adenocarcinoma in the gastric angle. A: The 70 kilo electron volt (kev) image in arterial phase (AP) show that the computed tomography attenuation value of 70 kev ($CT_{70\ kev}$) value of solid mass is 79.6 HU; B: The iodine map in AP show that the iodine concentration (IC) value of solid mass is 1.38 mg/mL; C: The effective atomic map in AP show that the effective atomic number (Z^{eff}) value of solid mass is 8.36; D: Histologic specimen shows a gastric adenocarcinoma of T4 staging in solid with HE staining (magnification, × 200); E: A 70 kev image in venous phase (VP) show that the $CT_{70\ kev}$ value of solid mass is 158.3 HU; F: An iodine map in VP show that the IC value of solid mass is 2.52 mg/mL; G: An effective atomic map in VP show that the Z^{eff} value of solid mass is 9.07; H: Ki-67 immunohistochemical staining demonstrated that approximately 40% of cells were positive for nuclear staining (magnification, × 400).

ARTICLE HIGHLIGHTS

Research background

The level of Ki-67 expression is a valuable prognostic factor in gastric cancer. However, the quantitative parameters based on the novel dual-layer spectral detector computed tomography (DLSDCT) in discriminating the Ki-67 expression status are unclear.

Research motivation

The relationship between the Ki-67 expression in gastric carcinoma (GC) and part spectral parameters (including the effective atomic number (Z^{eff}) and the monoenergetic CT attenuation) is unclear.

Research objectives

This study aimed to investigate the diagnostic ability of DLSDCT-derived parameters for Ki-67 expression status in GC.

Research methods

Dual-phase enhanced abdominal CT was performed preoperatively in 108 patients with GC. The monoenergetic CT attenuation value at 40-100 kilo electron volt (kev), the slope of the spectral curve (λ_{HU}), iodine concentration (IC), normalized IC (nIC), Z^{eff} and normalized Z^{eff} (nZ^{eff}) in the arterial phase (AP) and venous phase (VP) were retrospectively compared between the groups of low and high Ki-67 expression status. The relationship between the spectral parameters and Ki-67 expression status were analyzed, and the diagnostic efficacy of the statistically significant parameters between the two groups was compared.

Research results

The low and high Ki-67 expression groups consisted of 37 and 71 patients respectively. $CT_{40\ kev\text{-}VP}$, $CT_{70\ kev\text{-}VP}$, $CT_{100\ kev\text{-}VP}$, and Z^{eff}-related parameters were significantly higher, but IC-related parameters were lower in the low Ki-67 expression group than in the high Ki-67 expression group. $CT_{40\ kev\text{-}VP}$, $CT_{70\ kev\text{-}VP}$, $CT_{100\ kev\text{-}VP}$, Z^{eff}, and nZ^{eff} exhibited negative correlations with Ki-67 status, whereas IC and nIC positively correlated with it. The results of receiver operating characteristic analysis showed that the multi-variable model of spectral parameters performed well in identifying the Ki-67 status [area under the curve (AUC) = 0.967; sensitivity 95.77%; specificity 91.89%]. Nevertheless, the differentiating capabilities of single-variable model were moderate (AUC value from 0.630 to 0.835).

Research conclusions

Z^{eff} and IC may be useful parameters for evaluating the Ki-67 expression in GC.

Research perspectives

The spectral CT images are prospective to provide the pathological information of Ki-67 expression of GC in the future.

FOOTNOTES

Author contributions: Mao LT, Chen WC and Liu B designed the research; Lu JY, Zhang HL, Ye YS, and Deng WW collected the data; Mao LT and Liu X analyzed the data and wrote the manuscript; and all authors have read and approved the final manuscript.

Institutional review board statement: This retrospective study was approved by Institutional Review Board of our hospital (approval No.AF/04-07.0/10.0).

Informed consent statement: This informed consent was waived by Institutional Review Board of our hospital.

Conflict-of-interest statement: All the authors report no relevant conflicts of interest for this article.

Data sharing statement: No additional data are available.

Country/Territory of origin: China

ORCID number: Li-Ting Mao 0000-0003-2749-1850; Yong-Song Ye 0000-0003-1808-7418; Xian Liu 0000-0002-1662-477X.

S-Editor: Wang JJ
L-Editor: Ma JY-MedE
P-Editor: Wang JJ

REFERENCES

1 **Sung H**, Ferlay J, Siegel RL, Laversanne M, Soerjomataram I, Jemal A, Bray F. Global Cancer Statistics 2020: GLOBOCAN Estimates of Incidence and Mortality Worldwide for 36 Cancers in 185 Countries. *CA Cancer J Clin* 2021; **71**: 209-249 [PMID: 33538338 DOI: 10.3322/caac.21660]
2 **He Y**, Wang Y, Luan F, Yu Z, Feng H, Chen B, Chen W. Chinese and global burdens of gastric cancer from 1990 to 2019. *Cancer Med* 2021; **10**: 3461-3473 [PMID: 33931958 DOI: 10.1002/cam4.3892]
3 **He X**, Wu W, Lin Z, Ding Y, Si J, Sun LM. Validation of the American Joint Committee on Cancer (AJCC) 8th edition stage system for gastric cancer patients: a population-based analysis. *Gastric Cancer* 2018; **21**: 391-400 [PMID: 29052053 DOI: 10.1007/s10120-017-0770-1]
4 **Zhang H**, Pan Z, Du L, Yan C, Ding B, Song Q, Ling H, Chen K. Advanced gastric cancer and perfusion imaging using a multidetector row computed tomography: correlation with prognostic determinants. *Korean J Radiol* 2008; **9**: 119-127 [PMID: 18385558 DOI: 10.3348/kjr.2008.9.2.119]
5 **Xiong DD**, Zeng CM, Jiang L, Luo DZ, Chen G. Ki-67/MKI67 as a Predictive Biomarker for Clinical Outcome in Gastric Cancer Patients: an Updated Meta-analysis and Systematic Review involving 53 Studies and 7078 Patients. *J Cancer* 2019; **10**: 5339-5354 [PMID: 31632479 DOI: 10.7150/jca.30074]
6 **Scholzen T**, Gerdes J. The Ki-67 protein: from the known and the unknown. *J Cell Physiol* 2000; **182**: 311-322 [PMID: 10653597 DOI: 10.1002/(SICI)1097-4652(200003)182:3<311::AID-JCP1>3.0.CO;2-9]
7 **Wei Z**, Huang L, Zhang X, Xu A. Expression and significance of Her2 and Ki-67 in gastric adenocarcinoma without distant metastasis: a cohort study. *BMC Gastroenterol* 2020; **20**: 343 [PMID: 33059614 DOI: 10.1186/s12876-020-01484-9]
8 **Böger C**, Behrens HM, Röcken C. Ki67--An unsuitable marker of gastric cancer prognosis unmasks intratumoral heterogeneity. *J Surg Oncol* 2016; **113**: 46-54 [PMID: 26709194 DOI: 10.1002/jso.24104]
9 **Rassouli N**, Etesami M, Dhanantwari A, Rajiah P. Detector-based spectral CT with a novel dual-layer technology: principles and applications. *Insights Imaging* 2017; **8**: 589-598 [PMID: 28986761 DOI: 10.1007/s13244-017-0571-4]
10 **van Hamersvelt RW**, Willemink MJ, de Jong PA, Milles J, Vlassenbroek A, Schilham AMR, Leiner T. Feasibility and accuracy of dual-layer spectral detector computed tomography for quantification of gadolinium: a phantom study. *Eur Radiol* 2017; **27**: 3677-3686 [PMID: 28124106 DOI: 10.1007/s00330-017-4737-8]
11 **Hickethier T**, Baeßler B, Kroeger JR, Doerner J, Pahn G, Maintz D, Michels G, Bunck AC. Monoenergetic reconstructions for imaging of coronary artery stents using spectral detector CT: In-vitro experience and comparison to conventional images. *J Cardiovasc Comput Tomogr* 2017; **11**: 33-39 [PMID: 28096049 DOI: 10.1016/j.jcct.2016.12.005]
12 **Hickethier T**, Byrtus J, Hauger M, Iuga AI, Pahn G, Maintz D, Haneder S, Doerner J. Utilization of virtual mono-energetic

images (MonoE) derived from a dual-layer spectral detector CT (SDCT) for the assessment of abdominal arteries in venous contrast phase scans. *Eur J Radiol* 2018; **99**: 28-33 [PMID: 29362148 DOI: 10.1016/j.ejrad.2017.12.007]

13 **Meng X**, Ni C, Shen Y, Hu X, Chen X, Li Z, Hu D. Differentiating malignant from benign gastric mucosal lesions with quantitative analysis in dual energy spectral computed tomography: Initial experience. *Medicine (Baltimore)* 2017; **96**: e5878 [PMID: 28079827 DOI: 10.1097/MD.0000000000005878]

14 **Li R**, Li J, Wang X, Liang P, Gao J. Detection of gastric cancer and its histological type based on iodine concentration in spectral CT. *Cancer Imaging* 2018; **18**: 42 [PMID: 30413174 DOI: 10.1186/s40644-018-0176-2]

15 **Küpeli A**, Bulut E, Cansu A, Güner A, Soytürk M, Danışan G. Contribution of DECT in detecting serosal invasion of gastric cancer. *Turk J Med Sci* 2019; **49**: 782-788 [PMID: 31062940 DOI: 10.3906/sag-1811-168]

16 **Chen M**, Li X, Wei Y, Qi L, Sun YS. Spectral CT imaging parameters and Ki-67 labeling index in lung adenocarcinoma. *Chin J Cancer Res* 2020; **32**: 96-104 [PMID: 32194309 DOI: 10.21147/j.issn.1000-9604.2020.01.11]

17 **Wang P**, Tang Z, Xiao Z, Wu L, Hong R, Duan F, Wang Y, Zhan Y. Dual-energy CT in predicting Ki-67 expression in laryngeal squamous cell carcinoma. *Eur J Radiol* 2021; **140**: 109774 [PMID: 34004427 DOI: 10.1016/j.ejrad.2021.109774]

18 **Onishi S**, Fujioka C, Kaichi Y, Amatya VJ, Ishifuro M, Takeshima Y, Awai K, Sugiyama K, Kurisu K, Yamasaki F. Utility of dual-energy CT for predicting the vascularity of meningiomas. *Eur J Radiol* 2020; **123**: 108790 [PMID: 31864141 DOI: 10.1016/j.ejrad.2019.108790]

19 **Zhang X**, Bai L, Wang D, Huang X, Wei J, Zhang W, Zhang Z, Zhou J. Gastrointestinal stromal tumor risk classification: spectral CT quantitative parameters. *Abdom Radiol (NY)* 2019; **44**: 2329-2336 [PMID: 30980116 DOI: 10.1007/s00261-019-01973-w]

20 **Amin MB**, Edge SB, Greene FL, Byrd DR, Brookland RK, Washington MK, Gershenwald JE, Compton CC, Hess KR, Sullivan DC, Milburn Jessup J, Brierley JD, Gaspar LE, Schilsky RL, Balch CM, Winchester DP, Asare EA, Madera M, Gress DM, Meyer LR. AJCC cancer staging manual. Switzerland: Springer, 2017

21 **Li N**, Deng W, Ma J, Wei B, Guo K, Shen W, Zhang Y, Luo S. Prognostic evaluation of Nanog, Oct4, Sox2, PCNA, Ki67 and E-cadherin expression in gastric cancer. *Med Oncol* 2015; **32**: 433 [PMID: 25491144 DOI: 10.1007/s12032-014-0433-6]

22 **Cheng SM**, Ling W, Zhu J, Xu JR, Wu LM, Gong HX. Dual Energy Spectral CT Imaging in the assessment of Gastric Cancer and cell proliferation: A Preliminary Study. *Sci Rep* 2018; **8**: 17619 [PMID: 30514959 DOI: 10.1038/s41598-018-35712-w]

23 **Liang P**, Ren XC, Gao JB, Chen KS, Xu X. Iodine Concentration in Spectral CT: Assessment of Prognostic Determinants in Patients With Gastric Adenocarcinoma. *AJR Am J Roentgenol* 2017; **209**: 1033-1038 [PMID: 28871809 DOI: 10.2214/AJR.16.16895]

24 **Wang X**, Liu D, Zeng X, Jiang S, Li L, Yu T, Zhang J. Dual-energy CT quantitative parameters for evaluating Immunohistochemical biomarkers of invasive breast cancer. *Cancer Imaging* 2021; **21**: 4 [PMID: 33413654 DOI: 10.1186/s40644-020-00370-7]

25 **Taylor ML**. Quantification of differences in the effective atomic numbers of healthy and cancerous tissues: a discussion in the context of diagnostics and dosimetry. *Med Phys* 2012; **39**: 5437-5445 [PMID: 22957611 DOI: 10.1118/1.4742849]

26 **Gorshkov V**, Rozhkova N, Prokopenko S. Dual-energy dividing mammography. Berlin, Heidelberg: Springer, 2010

27 **Reddy SB**, John Charles M, Naga Raju GJ, Vijayan V, Seetharami Reddy B, Ravi Kumar M, Sundareswar B. Trace elemental analysis of carcinoma kidney and stomach by PIXE method. *Nucl Instrum Methods Phys Res B* 2003; **207**: 345-355 [DOI: 10.1016/S0168-583X(03)00463-4]

28 **Yaman M**. Comprehensive comparison of trace metal concentrations in cancerous and non-cancerous human tissues. *Curr Med Chem* 2006; **13**: 2513-2525 [PMID: 17017908 DOI: 10.2174/092986706778201620]

29 **Hu S**, Huang W, Chen Y, Song Q, Lin X, Wang Z, Chen K. Spectral CT evaluation of interstitial brachytherapy in pancreatic carcinoma xenografts: preliminary animal experience. *Eur Radiol* 2014; **24**: 2167-2173 [PMID: 24903229 DOI: 10.1007/s00330-014-3257-z]

30 **Thaiss WM**, Haberland U, Kaufmann S, Spira D, Thomas C, Nikolaou K, Horger M, Sauter AW. Iodine concentration as a perfusion surrogate marker in oncology: Further elucidation of the underlying mechanisms using Volume Perfusion CT with 80 kVp. *Eur Radiol* 2016; **26**: 2929-2936 [PMID: 26679179 DOI: 10.1007/s00330-015-4154-9]

31 **Wang SH**, Sun YF, Liu Y, Zhou Y. CT contrast enhancement correlates with pathological grade and microvessel density of pancreatic cancer tissues. *Int J Clin Exp Pathol* 2015; **8**: 5443-5449 [PMID: 26191248]

32 **Wu J**, Lv Y, Wang N, Zhao Y, Zhang P, Liu Y, Chen A, Li J, Li X, Guo Y, Wu T, Liu A. The value of single-source dual-energy CT imaging for discriminating microsatellite instability from microsatellite stability human colorectal cancer. *Eur Radiol* 2019; **29**: 3782-3790 [PMID: 30903331 DOI: 10.1007/s00330-019-06144-5]

Published by **Baishideng Publishing Group Inc**
7041 Koll Center Parkway, Suite 160, Pleasanton, CA 94566, USA
Telephone: +1-925-3991568
E-mail: bpgoffice@wjgnet.com
Help Desk: https://www.f6publishing.com/helpdesk
https://www.wjgnet.com